Lipoatrophic diabetes in *Irs1*$^{-/-}$/*Irs3*$^{-/-}$ double knockout mice

Palle G. Laustsen,[1,3] M. Dodson Michael,[1,3] Barbara E. Crute,[2] Shmuel E. Cohen,[1] Kohjiro Ueki,[1] Rohit N. Kulkarni,[1] Susanna R. Keller,[2] Gustav E. Lienhard,[2] and C. Ronald Kahn[1,4]

[1]Joslin Diabetes Center and Department of Medicine, Harvard Medical School, Boston, Massachusetts 02215, USA; [2]Department of Biochemistry, Dartmouth Medical School, Hanover, New Hampshire 03755, USA

Based on the phenotypes of knockout mice and cell lines, as well as pathway-specific analysis, the insulin receptor substrates IRS-1, IRS-2, IRS-3, and IRS-4 have been shown to play unique roles in insulin signal transduction. To investigate possible functional complementarity within the IRS family, we generated mice with double knockout of the genes for IRS-1/IRS-3 and IRS-1/IRS-4. Mice with a combined deficiency of IRS-1 and IRS-4 showed no differences from *Irs1*$^{-/-}$ mice with respect to growth and glucose homeostasis. In contrast, mice with a combined deficiency of IRS-1 and IRS-3 developed early-onset severe lipoatrophy associated with marked hyperglycemia, hyperinsulinemia, and insulin resistance. However, in contrast to other models of lipoatrophic diabetes, there was no accumulation of fat in liver or muscle. Furthermore, plasma leptin levels were markedly decreased, and adenovirus-mediated expression of leptin in liver reversed the hyperglycemia and hyperinsulinemia. The results indicate that IRS-1 and IRS-3 play important complementary roles in adipogenesis and establish the *Irs1*$^{-/-}$/*Irs3*$^{-/-}$ double knockout mouse as a novel model of lipoatrophic diabetes.

[*Keywords*: Lipoatrophic diabetes; adipogenesis; leptin; insulin receptor substrate]

Received August 20, 2002; revised version accepted October 18, 2002.

The insulin receptor substrate (IRS) family of proteins plays a central role in insulin signal transduction. Following activation of the insulin receptor kinase, IRS-1, IRS-2, IRS-3, and IRS-4 undergo phosphorylation of multiple tyrosine residues in unique sequence motifs throughout the molecule. Many of these tyrosine phosphorylated residues serve as recognition sites for Src-homology-2 (SH-2) domain-containing proteins, including the p85 regulatory subunit of phosphatidylinositol 3 (PI 3)-kinase, Grb2, Fyn, and SHP-2 (Saltiel and Kahn 2001). Phosphorylation on tyrosine and serine also promotes binding of other proteins, such as SERCA 1 and SERCA 2, the 14-3-3 proteins, and the SV40 large T-antigen, via other mechanisms (Virkamaki et al. 1999). The association of each of these with the IRS proteins provokes changes in subcellular location and trafficking and/or enzyme activity that serve to transmit the insulin signal downstream, ultimately leading to the hormone's cellular effects on glucose uptake, protein synthesis, and regulation of specific gene expression (Saltiel and Kahn 2001).

The existence of four homologous IRS molecules raises the question of the physiological role of each and to what extent there is complementarity or overlap in the physiological roles. Studies of mice with targeted disruption of the *Irs* genes lend some support to both situations. *Irs1* knockout (*Irs1*$^{-/-}$) mice show significant embryonic and postnatal growth retardation, suggesting that IRS-1 plays a key role in relaying the growth-stimulating effects of insulin and insulin-like growth factor (IGF; Araki et al. 1994; Tamemoto et al. 1994). IRS-1-deficient mice also have insulin resistance and mild glucose intolerance, but do not develop diabetes. *Irs2*$^{-/-}$ mice, on the other hand, are only slightly smaller than wild-type mice. The absence of IRS-2 also produces insulin resistance, and in addition, a defect in β-cell proliferation. This results in insufficient insulin secretion to compensate for the insulin resistance, thus leading to diabetes at a young age (Withers et al. 1998; Kubota et al. 2000). In cell culture models, IRS-1 and IRS-2 also produce different phenotypes. For example, in cultured brown preadipocytes, loss of IRS-1 results in a failure of differentiation and lipid accumulation, whereas loss of IRS-2 results in a defect in insulin-stimulated glucose transport, despite normal differentiation (Fasshauer et al. 2000, 2001). These observations indicate that IRS-1 and IRS-2, which are the major insulin receptor substrates expressed in all tissues, play significant and nonredundant roles in growth and regulation of glucose homeostasis.

IRS-3 and IRS-4 show a restricted tissue distribution and are less clear in terms of function. IRS-3 is most abundant in adipocytes, and its mRNA is also detected

[3]These authors contributed equally to this work.
[4]Corresponding author.
E-MAIL c.ronald.kahn@joslin.harvard.edu; FAX (617) 732-2487.
Article and publication are at http://www.genesdev.org/cgi/doi/10.1101/gad.1034802.

in liver, heart, lung, and kidney (Sciacchitano and Taylor 1997). However, in contrast to the severe phenotypes observed in *Irs1*$^{-/-}$ and *Irs2*$^{-/-}$ mice, disruption of the gene for IRS-3 does not result in any detectable abnormalities in growth or glucose homeostasis (Liu et al. 1999). IRS-4 mRNA is present in skeletal muscle, liver, heart, hypothalamus, and kidney (Fantin et al. 1999), and *Irs4*$^{-/-}$ mice show only very modest growth retardation and slight glucose intolerance (Fantin et al. 2000). Although one interpretation of these findings is that IRS-3 and IRS-4 are not critically involved in regulating growth and glucose homeostasis, another possibility is that IRS-1 and/or IRS-2 functionally compensate for the absence of IRS-3 or IRS-4. Similarly, it is possible that IRS-3 and IRS-4 ameliorate the phenotypes of *Irs1*$^{-/-}$ and *Irs2*$^{-/-}$ mice.

To investigate to what extent functional complementarity or redundancy occurs within the IRS family, we generated mice lacking genes for two IRS proteins, either IRS-1 and IRS-3 or IRS-1 and IRS-4. Here we show that combined deficiency of IRS-1 and IRS-3 results in severe lipoatrophy, indicating that these IRS proteins are critical for and functionally interchangeable in adipogenesis. In contrast, we found no evidence for a functional overlap between IRS-1 and IRS-4.

Results

Growth and development of Irs *double knockout mice*

Mice with a combined deficiency of IRS-1 and IRS-3 were generated by interbreeding of *Irs1*$^{+/-}$/*Irs3*$^{+/-}$ animals. This breeding strategy also generated wild-type, *Irs1*$^{-/-}$, and *Irs3*$^{-/-}$ mice, the phenotypes of which were compared with that of *Irs1*$^{-/-}$/*Irs3*$^{-/-}$ double knockout mice throughout the study. In these breedings, *Irs1*$^{-/-}$/*Irs3*$^{-/-}$ double knockout progeny were observed at about half the expected frequency based on a Mendelian distribution (3.4% vs. 6.25%), suggesting increased prenatal and/or early postnatal lethality of the *Irs1*$^{-/-}$/*Irs3*$^{-/-}$ double knockout mice. The growth curves for the surviving *Irs1*$^{-/-}$/*Irs3*$^{-/-}$ double knockout male and female mice overlapped with those for *Irs1*$^{-/-}$ mice, showing severe generalized growth retardation throughout life compared with wild-type control mice (Fig. 1A). *Irs3*$^{-/-}$ mice tended to be slightly smaller than wild-type control mice, but the differences were not statistically significant.

To obtain mice lacking both IRS-1 and IRS-4, *Irs1*$^{+/-}$/*Irs4*$^{+/-}$ females were bred with *Irs1*$^{+/-}$/*Irs4*$^{-}$ males. Because the *Irs4* gene is on the mouse X chromosome, this breeding scheme produced *Irs1*$^{-/-}$/*Irs4*$^{-}$ double knockout male and *Irs1*$^{-/-}$/*Irs4*$^{-/-}$ double knockout female mice (hereafter collectively referred to as *Irs1*$^{-/-}$/*Irs4*$^{-/-}$ double knockout mice), *Irs1*$^{-/-}$ mice (males) and *Irs1*$^{-/-}$/*Irs4*$^{+/-}$ mice (females). Throughout the study, the phenotypes of the latter two were compared with those of the *Irs1*$^{-/-}$/*Irs4*$^{-/-}$ double knockout males and females, respectively. Absence of IRS-4 was previously shown to impose a mild growth defect on male mice (Fantin et al. 2000). On the *Irs1*$^{-/-}$ background, however, the absence of IRS-4 caused no additional defect in growth of either sex (data not shown), confirming IRS-1 as the major IRS involved in growth.

Irs1$^{-/-}$/Irs3$^{-/-}$ *double knockout mice are lipoatrophic*

Dissection of *Irs1*$^{-/-}$/*Irs3*$^{-/-}$ double knockout mice revealed an obvious generalized deficiency of white adipose tissue (Fig. 1B). Perigonadal fat pad mass was reduced by ~95%, ~80%, and ~85% as compared with those of wild-type, *Irs1*$^{-/-}$, and *Irs3*$^{-/-}$ mice, respectively (Fig. 1C). Whole-body triglyceride content of the *Irs1*$^{-/-}$/*Irs3*$^{-/-}$ double knockout mice was also severely reduced by ~75%, ~45%, and ~70% from that of wild-type, *Irs1*$^{-/-}$, and *Irs3*$^{-/-}$ mice, respectively (Fig. 1E). Histologic analysis with measurement of adipocyte diameter showed that the cells of perigonadal fat pads from *Irs1*$^{-/-}$/*Irs3*$^{-/-}$ double knockout mice were smaller than those of fat pads from wild-type, *Irs1*$^{-/-}$, and *Irs3*$^{-/-}$ mice (Fig. 1F). Northern blot analysis of RNA extracted from epididymal fat pads showed a marked reduction in mRNA coding for peroxisome proliferator activated receptor γ (PPARγ), a marker of fully differentiated adipocytes, in *Irs1*$^{-/-}$/*Irs3*$^{-/-}$ double knockout mice (Fig. 1G). In contrast to the marked reduction in white adipose tissue mass, the interscapular brown fat pad was normal in color and size (Fig. 1B,D). Thus, loss of IRS-1 and IRS-3 selectively interferes with formation of white adipose tissue.

Corresponding with the reduced white adipose tissue mass, fed plasma leptin levels were lower in the *Irs1*$^{-/-}$/*Irs3*$^{-/-}$ double knockout mice (Fig. 2A). Fasted plasma leptin was also reduced, although less pronounced than in the fed state (Fig. 2B). Furthermore, fasted plasma triglyceride levels were significantly lower in *Irs1*$^{-/-}$/*Irs3*$^{-/-}$ double knockout male mice and female mice compared with wild-type and *Irs3*$^{-/-}$ mice and in female mice also when compared with *Irs1*$^{-/-}$ mice (Fig. 2C). Also, fasted plasma free fatty acid levels were significantly reduced in both male and female *Irs1*$^{-/-}$/*Irs3*$^{-/-}$ double knockout mice compared with wild-type mice and in male mice also when compared with *Irs1*$^{-/-}$ and *Irs3*$^{-/-}$ mice (Fig. 2D).

The deficiency of adipose tissue was not associated with increased deposition of fat in liver, because the livers of *Irs1*$^{-/-}$/*Irs3*$^{-/-}$ double knockout mice appeared normal in color and tended to contain less triglyceride than did livers of wild-type control mice (Fig. 2E), although this was not statistically significant. Likewise, the triglyceride content of skeletal muscle was not statistically different from that of wild-type mice.

In contrast with the *Irs1*$^{-/-}$/*Irs3*$^{-/-}$ double knockout mice, we did not observe any changes in organ sizes in the *Irs1*$^{-/-}$/*Irs4*$^{-/-}$ double knockout mice compared with *Irs1*$^{-/-}$ mice.

Metabolic parameters

Irs1$^{-/-}$/*Irs3*$^{-/-}$ double knockout mice displayed elevated blood glucose levels as early as 5 wk after birth in both

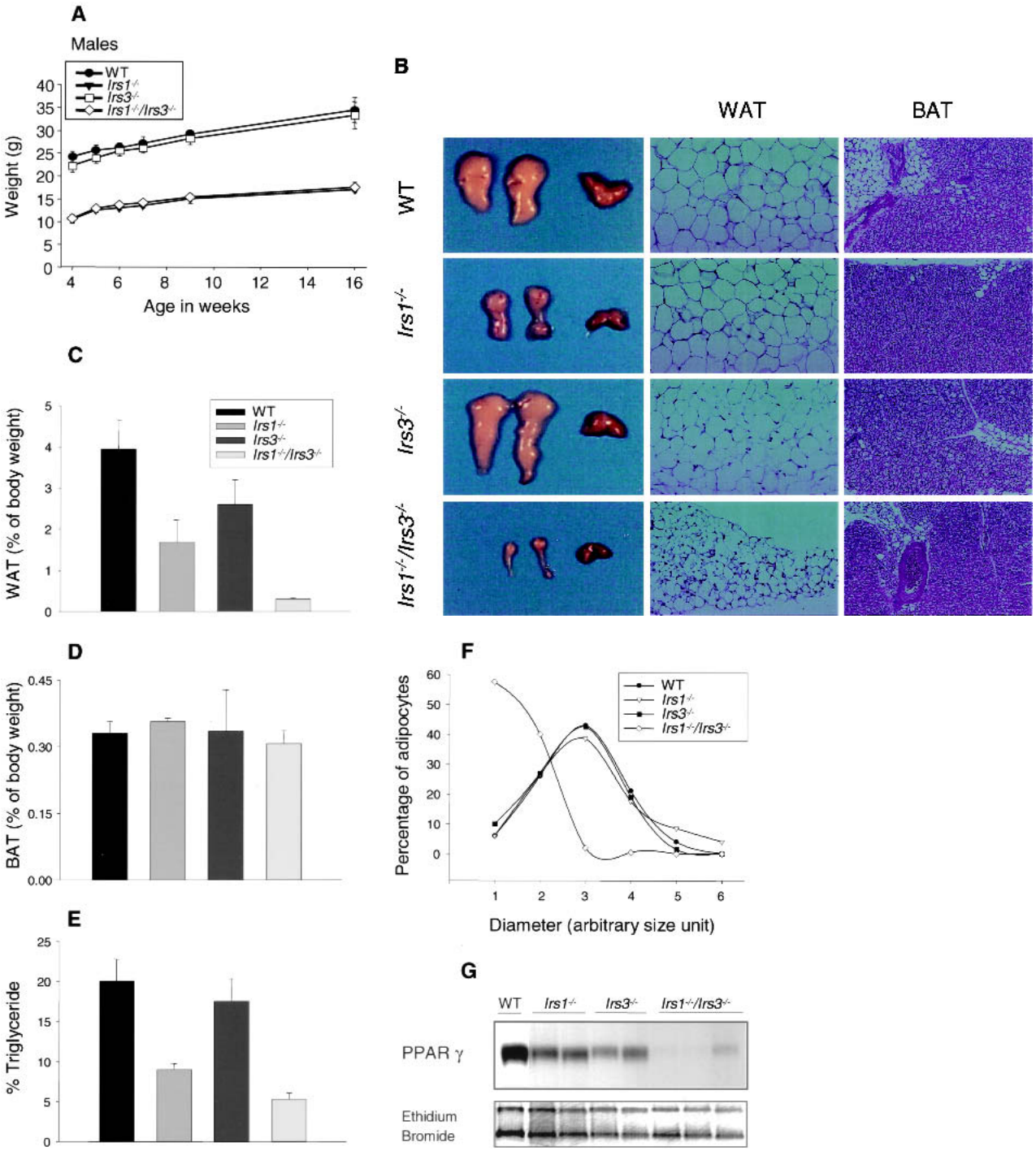

Figure 1. *Irs1*$^{-/-}$/*Irs3*$^{-/-}$ double knockout mice are lipoatrophic. (*A*) Growth curves. Body weights for wild-type, *Irs1*$^{-/-}$, *Irs3*$^{-/-}$, and *Irs1*$^{-/-}$/*Irs3*$^{-/-}$ double knockout male mice were determined at indicated time points between the ages of 4 and 16 wk. Growth curves for female mice followed a similar pattern (data not shown). (*B*) Photographs of epididymal and interscapular fat pads isolated from wild-type (WT), *Irs1*$^{-/-}$, *Irs3*$^{-/-}$, and *Irs1*$^{-/-}$/*Irs3*$^{-/-}$ double knockout mice (*left* panel). Sections of white adipose tissue (WAT) are shown at 40× magnification (*middle* panel) and of brown adipose tissue (BAT) at 10× magnification (*right* panel). (*C*) Perigonadal fat pad weight as percentage of total body weight. Data in *C–E* are shown as means ± S.E. (*D*) Interscapular fat pad weight as percentage of total body weight. (*E*) Total body triglyceride content as percentage of total body weight. (*F*) Cell size distribution in perigonadal fat pads was analyzed from tissue sections as described in Materials and Methods. (*G*) Reduced expression of *PPARγ* in epididymal fat pads. Northern blot of total RNA isolated from epididymal fat pads probed with a ^{32}P-labeled PPARγ cDNA fragment. Each lane represents a single animal.

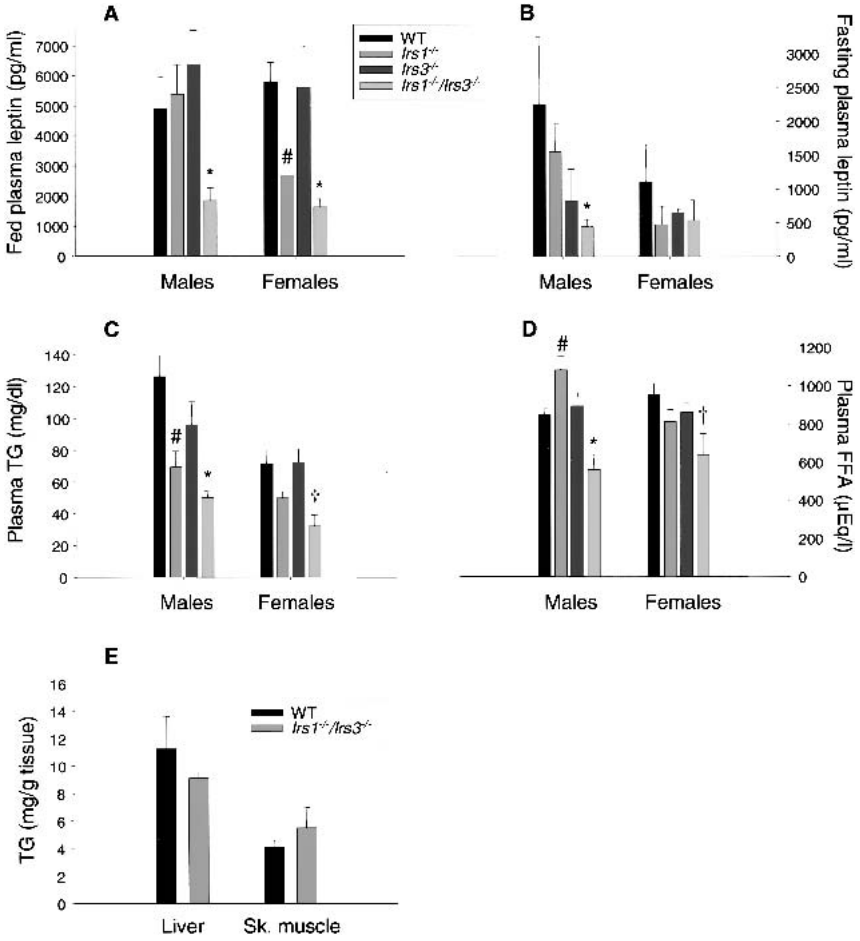

Figure 2. Reduced leptin, free fatty acid, and triglyceride plasma levels in $Irs1^{-/-}/Irs3^{-/-}$ double knockout mice. (*A*) Plasma leptin levels were measured in random-fed mice (n = 3–5). *, $P < 0.05$ for $Irs1^{-/-}/Irs3^{-/-}$ versus WT, $Irs1^{-/-}$, and $Irs3^{-/-}$ mice. #, $P < 0.05$ for $Irs1^{-/-}$ versus WT mice. (*B*) Plasma leptin levels in mice after overnight fast (n = 2–5). *, $P < 0.05$ for $Irs1^{-/-}/Irs3^{-/-}$ versus $Irs1^{-/-}$ mice. (*C*) Plasma triglyceride (TG) levels after overnight fast (n = 6–14). *, $P < 0.05$ for $Irs1^{-/-}/Irs3^{-/-}$ versus WT and $Irs3^{-/-}$ mice. #, $P < 0.01$ for $Irs1^{-/-}$ versus WT mice. †, $P < 0.01$ for $Irs1^{-/-}/Irs3^{-/-}$ versus WT, $Irs1^{-/-}$, and $Irs3^{-/-}$ mice. (*D*) Plasma free fatty acid levels after overnight fast (n = 3–5). *, $P < 0.05$ for $Irs1^{-/-}/Irs3^{-/-}$ versus WT, $Irs1^{-/-}$, and $Irs3^{-/-}$ mice. #, $P < 0.05$ for $Irs1^{-/-}$ versus WT mice. †, $P < 0.01$ for $Irs1^{-/-}/Irs3^{-/-}$ versus WT mice. In *A–D*, data are shown as means ± S.E. for the indicated number of animals. All data were from 2-month-old mice. (*E*) Liver and skeletal muscle triglyceride content. The total glycerol content of liver and skeletal muscle was determined after incubation of tissue homogenates with lipoprotein lipase. Values were converted into milligrams of triglyceride per gram of tissue (wet weight) after comparison with a glycerol standard (Sigma). Liver and skeletal muscle were removed from 4-month-old, random-fed male mice (n = 6 in each group). Data are shown as means ± S.E.

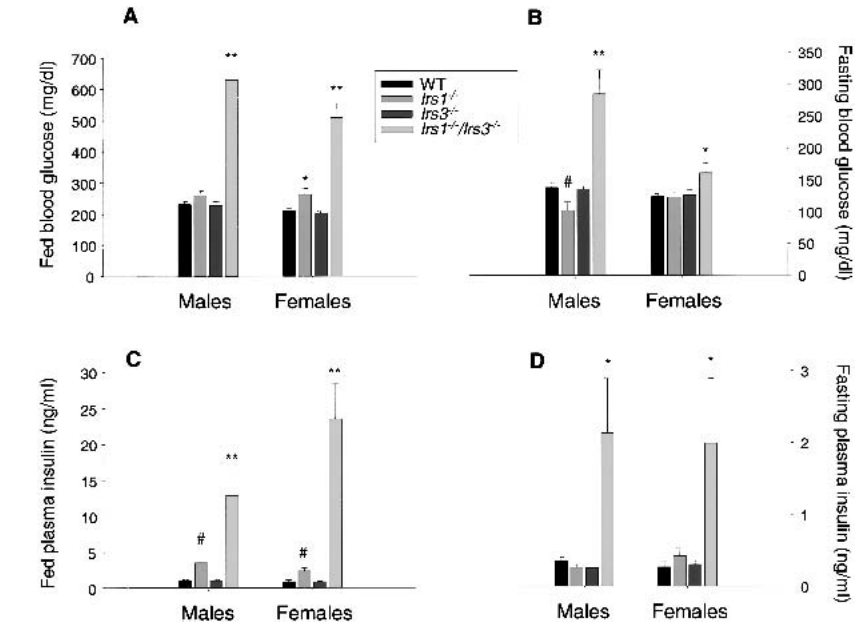

Figure 3. $Irs1^{-/-}/Irs3^{-/-}$ double knockout mice are hyperglycemic and hyperinsulinemic. (*A*) Blood glucose levels in 2-month-old random-fed mice (n = 6–11 in each group). **, $P < 0.001$ for $Irs1^{-/-}/Irs3^{-/-}$ versus WT, $Irs1^{-/-}$, and $Irs3^{-/-}$ mice. *, $P < 0.05$ for $Irs1^{-/-}$ versus WT and $Irs3^{-/-}$ mice. (*B*) Blood glucose in 2-month-old mice after overnight fast (n = 6–14). **, $P < 0.001$ for $Irs1^{-/-}/Irs3^{-/-}$ versus WT, $Irs1^{-/-}$, and $Irs3^{-/-}$ mice. *, $P < 0.05$ for $Irs1^{-/-}/Irs3^{-/-}$ versus WT, $Irs3^{-/-}$ mice. #, $P < 0.05$ for $Irs1^{-/-}$ versus WT and $Irs3^{-/-}$ mice. (*C*) Plasma insulin levels in 2-month-old random-fed mice (n = 6–14). **, $P < 0.001$ for $Irs1^{-/-}/Irs3^{-/-}$ versus WT and $Irs3^{-/-}$ mice. $P < 0.05$ for $Irs1^{-/-}/Irs3^{-/-}$ versus $Irs1^{-/-}$ mice. #, $P < 0.01$ for $Irs1^{-/-}$ versus WT and $Irs3^{-/-}$ mice. (*D*) Plasma insulin levels in 2-month-old mice after overnight fast (n = 6–14). *, $P < 0.05$ for $Irs1^{-/-}/Irs3^{-/-}$ versus WT and $Irs3^{-/-}$ mice; for male mice, also versus $Irs1^{-/-}$ mice. In *A–D*, data are shown as means ± S.E. for the indicated number of mice.

the fasted and the fed states (Fig. 3A,B). The hyperglycemia occurred despite markedly elevated plasma insulin levels in both the fasted and fed states (Fig. 3C,D), correlating with an increase in pancreatic β-cell mass (see below). Intraperitoneal glucose tolerance tests demonstrated marked glucose intolerance in *Irs1*$^{-/-}$/*Irs3*$^{-/-}$ double knockout mice (Fig. 4A,B). Furthermore, insulin tolerance tests showed that *Irs1*$^{-/-}$/*Irs3*$^{-/-}$ double knockout mice were severely resistant to the glucose-lowering effect of exogenous insulin (Fig. 4C,D). Thus, *Irs1*$^{-/-}$/*Irs3*$^{-/-}$ double knockout mice represent a novel model of lipoatrophic diabetes with markedly reduced fat mass, reduced leptin levels, severe insulin resistance, and hyperinsulinemia.

In contrast to the severe defects in glucose homeostasis in the *Irs1*$^{-/-}$/*Irs3*$^{-/-}$ double knockout mice, no differences were observed between *Irs1*$^{-/-}$/*Irs4*$^{-/-}$ double knockout and *Irs1*$^{-/-}$ mice in terms of fed and fasted blood glucose levels and fed and fasted plasma insulin levels (Table 1). Furthermore, *Irs1*$^{-/-}$/*Irs4*$^{-/-}$ double knockout and *Irs1*$^{-/-}$ mice responded similarly when subjected to glucose tolerance tests (Fig. 5A,B) and insulin tolerance tests (Fig. 5C,D).

Analysis of β-cell mass

As previously reported (Kulkarni et al. 1999; Flier et al. 2001), *Irs1*$^{-/-}$ mice exhibit a significant ~twofold increase in β-cell mass when compared with wild-type control mice, reflecting the effect of systemic insulin resistance and/or the effect of a circulating islet growth factor on islet hyperplasia (Fig. 6A,B). In contrast, the *Irs3*$^{-/-}$ mice have a normal β-cell mass. In agreement with the marked hyperinsulinemia, both male and female *Irs1*$^{-/-}$/*Irs3*$^{-/-}$ double knockout mice showed a severe islet hyperplasia with a 4.3-fold increase compared with wild-type control and *Irs3*$^{-/-}$ mice, and a 1.9-fold increase when compared with *Irs1*$^{-/-}$ mice alone (Fig. 6A,B). No significant differences were observed in the mass or distribution of non-β-cells between the various groups.

Reversal of diabetes in Irs1$^{-/-}$/Irs3$^{-/-}$ *double knockout mice by adenovirus-mediated expression of leptin*

Infusion of recombinant leptin has previously been shown to overcome insulin resistance in the aP2-nSREBP-1c mouse, a transgenic mouse model of congenital lipodystrophy with moderate reduction in white adipose tissue mass (Shimomura et al. 1999). In another and more severe model of lipoatrophic diabetes, the A-ZIP/F-1 transgenic mouse, leptin infusion also reversed the diabetic phenotype although only at very high plasma leptin levels (Gavrilova et al. 2000; Ebihara et al. 2001). To test if leptin treatment would reverse diabetes in the *Irs1*$^{-/-}$/*Irs3*$^{-/-}$ double knockout mice, recombinant adenovirus carrying leptin cDNA was injected into *Irs1*$^{-/-}$/*Irs3*$^{-/-}$ double knockout mice as well as wild-type and leptin-deficient *ob/ob* control mice. In each case, the effect of injecting leptin adenovirus was compared with the effect of injecting adenovirus carrying the gene for bacterial β-galactosidase. As expected, *ob/ob* mice responded to leptin treatment with a normalization of blood glucose and plasma insulin levels (Fig. 7A,B). Leptin treatment had no significant effect on these parameters in wild-type mice. In the *Irs1*$^{-/-}$/*Irs3*$^{-/-}$ double knockout mice, injection of leptin adenovirus led to normalization of blood glucose and plasma insulin levels. Plasma leptin levels in *Irs1*$^{-/-}$/*Irs3*$^{-/-}$ double knockout mice injected with leptin adenovirus were on average increased approximately twofold compared with ani-

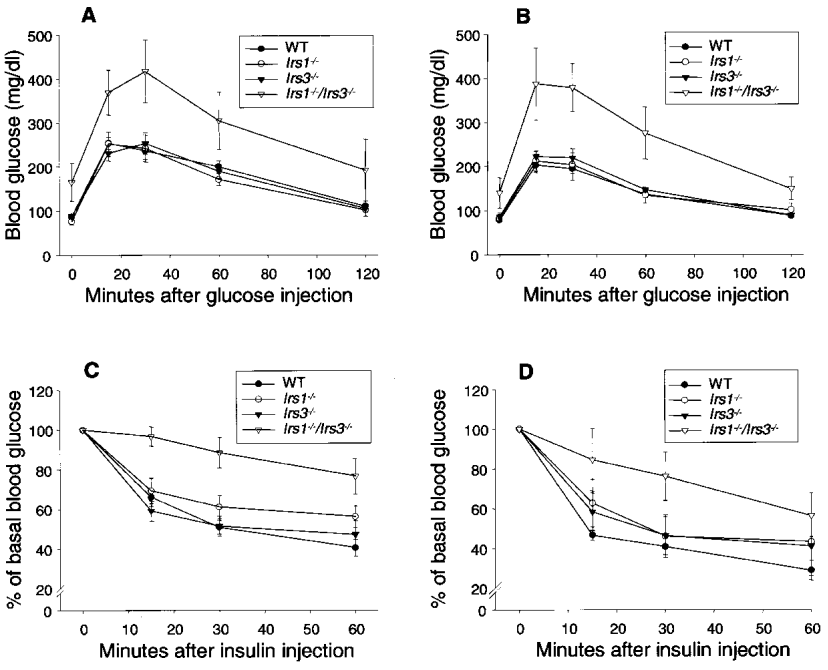

Figure 4. *Irs1*$^{-/-}$/*Irs3*$^{-/-}$ double knockout mice are insulin-resistant and glucose-intolerant. (*A*,*B*) Glucose tolerance tests. Glucose levels were determined in 6-week-old male (*A*) and female (*B*) mice immediately before and at the indicated time points after intraperitoneal injection of glucose (2 g/kg body weight). Each point represents the mean ± S.E. for 5–8 animals. (*C*,*D*) Insulin tolerance tests. Glucose levels were determined in 6-week-old male (*C*) and female (*D*) mice immediately before and at the indicated time points after intraperitoneal injection of human insulin (1 U/kg body weight). Each point represents the mean ± S.E. for 6–8 animals.

Table 1. *Blood glucose and plasma insulin levels for* Irs1$^{-/-}$ *and* Irs1$^{-/-}$/Irs4$^{-/-}$ *mice*

	Males		Females	
	Irs1$^{-/-}$	*Irs1*$^{-/-}$/*Irs4*$^{-}$	*Irs1*$^{-/-}$	*Irs1*$^{-/-}$/*Irs4*$^{-/-}$
Blood glucose (mg/dL)				
Fasted	59.9 ± 5.4	61.1 ± 5.1	43.5 ± 2.7	46.1 ± 3.7
Fed	113 ± 4.1	121.9 ± 3.8	95.2 ± 5.6	102.9 ± 6.4
Plasma insulin (ng/mL)				
Fasted	0.36 ± 0.08	0.27 ± 0.08	0.43 ± 0.08	0.33 ± 0.12
Fed	1.55 ± 0.41	2.21 ± 0.89	1.25 ± 0.23	1.03 ± 0.18

Results are shown as mean ± S.E. for 6–14 animals in each group. All data were from 10–17-week-old mice.

mals injected with control adenovirus (0.92 ± 0.33 vs. 0.44 ± 0.16 ng/mL), although this was not statistically significant. Leptin treatment was associated with a further reduction in white adipose tissue mass as perigonadal fat pads could not be identified in three out of four *Irs1*$^{-/-}$/*Irs3*$^{-/-}$ double knockout mice injected with leptin adenovirus versus in one out of four animals injected with control virus. Body weight changes were –0.28 ± 0.59 g and 0.18 ± 0.19 g for *Irs1*$^{-/-}$/*Irs3*$^{-/-}$ double knockout mice injected with leptin adenovirus and with control virus, respectively, but the difference was not statistically significant. Taken together, these data suggest that the diabetic phenotype of *Irs1*$^{-/-}$/*Irs3*$^{-/-}$ double knockout mice was caused, at least in part, by leptin deficiency as a result of reduced white adipose tissue mass.

Discussion

The insulin and IGF-1 receptors are unique among other members of the receptor tyrosine kinase superfamily relying on phosphorylation and docking of SH2-domain-containing proteins to intracellular substrates rather than the receptor itself. Indeed, more than nine different insulin receptor substrates have been identified, and four of them fall into the family of IRS proteins (Saltiel and Kahn 2001). The existence of families composed of highly homologous proteins raises the question of the physiological role of each family member. It also raises the question as to whether other family members can functionally complement or compensate for one another, and to what extent there is functional redundancy.

Within the IRS protein family, studies of single-gene knockout mice have indicated both unique, and partly overlapping, physiological roles for IRS-1 and IRS-2, whereas IRS-3 and IRS-4 seem to be less important or perhaps redundant in terms of the effects of insulin on growth, development, and glucose homeostasis, because knockout of these genes has little apparent phenotype. However, in the present study we show that mice with a combined deficiency of IRS-1 and IRS-3 develop early-onset lipoatrophy associated with marked hyperglycemia, hyperinsulinemia, insulin resistance, glucose intolerance, and islet hyperplasia. Thus, IRS-3 does have a physiological function in metabolism and development of white adipose tissue, and plays a very important role in mice lacking IRS-1.

The finding that the perigonadal fat pads consisted of

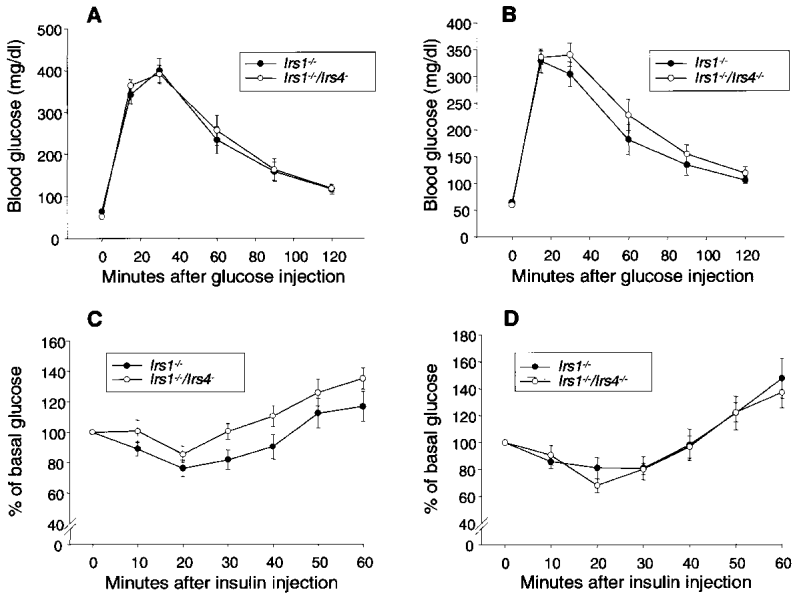

Figure 5. *Irs1*$^{-/-}$/*Irs4*$^{-/-}$ mice and *Irs1*$^{-/-}$ mice show similar responses to glucose tolerance and insulin tolerance tests. (*A*,*B*) Glucose tolerance tests. Glucose levels were determined in 9–12-week-old male (*A*) and female (*B*) mice immediately before and at the indicated time points after intraperitoneal injection of glucose (2 g/kg body weight). Each point represents the mean ± S.E. for seven animals. (*C*,*D*) Insulin tolerance tests. Glucose levels were determined in 9–12-week-old male (*C*) and female (*D*) mice immediately before and at the indicated time points after intraperitoneal injection of human insulin (0.75 U/kg body weight). Each point represents the mean ± S.E. for 6–8 animals.

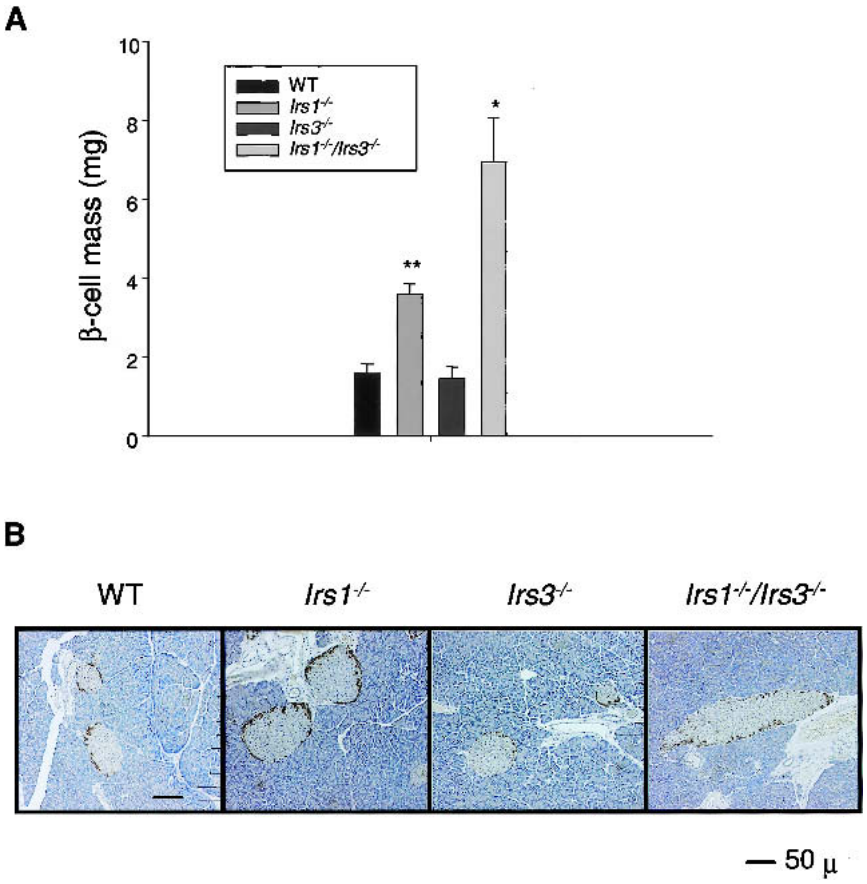

Figure 6. *Irs1*$^{-/-}$/*Irs3*$^{-/-}$ double knockout mice show β-cell hyperplasia. (*A*) β-cell mass was determined as described in Materials and Methods. For each group, n = 4–5 males, except for the *Irs1*$^{-/-}$/*Irs3*$^{-/-}$ group, in which n = 4 (2 males and 2 females). Data are shown as means ± SE. *, $P < 0.05$ for *Irs1*$^{-/-}$/*Irs3*$^{-/-}$ versus WT, *Irs1*$^{-/-}$, and *Irs3*$^{-/-}$ mice. **, $P < 0.001$ for *Irs1*$^{-/-}$ versus WT and *Irs3*$^{-/-}$ mice. (*B*) Representative sections from pancreas from 2-month-old WT, *Irs1*$^{-/-}$, *Irs3*$^{-/-}$, and *Irs1*$^{-/-}$/*Irs3*$^{-/-}$ double knockout male mice. Sections were stained with a cocktail of antibodies against the non-β-cells and counterstained with hematoxylin as described in Materials and Methods. Magnification, 10×. Bar, 50 μm.

small and PPARγ-deficient cells indicated that the lipoatrophy was caused by defective adipogenesis. Insulin is required for efficient differentiation of preadipocyte cell lines and promotes lipid accumulation. In vitro, insulin has been suggested to signal through the IGF-1 receptor to promote preadipocyte differentiation, explaining why pharmacological doses of insulin are required in differentiation protocols (Rosen and Spiegelman 2000). However, cultured brown preadipocytes lacking the insulin receptor fail to differentiate, indicating an essential role of the insulin receptor in adipogenesis (A. Entingh and C. Ronald Kahn, unpubl.).

IRS proteins are known substrates for the IGF-1 receptor, as well as the insulin receptor, thus IRS-1 and IRS-3 may be involved in relaying the prodifferentiation signal of either growth hormone. IRS-1 has been shown to be required for differentiation of brown preadipocyte cell lines, supporting a role for IRS proteins in adipocyte differentiation (Fasshauer et al. 2001). However, *Irs1*$^{-/-}$ mice have normal brown adipose tissue mass and normally appearing, although reduced in amount, white adipose tissue, suggesting that alternative, IRS-1-independent pathway(s) are able to drive adipocyte differentiation in vivo. Our data suggest that IRS-3 may function as an alternative substrate for insulin and IGF-1 receptors in differentiation of white preadipocytes in the *Irs1*$^{-/-}$ mouse. However, *Irs1*$^{-/-}$/*Irs3*$^{-/-}$ double knockout mice have normal brown adipose tissue mass, indicating that other pathways can promote differentiation of brown preadipocytes in vivo.

Plasma insulin levels were markedly elevated in *Irs1*$^{-/-}$/*Irs3*$^{-/-}$ double knockout mice compared with all three control groups, including *Irs1*$^{-/-}$ mice, which also show hyperinsulinemia and peripheral insulin resistance (Araki et al. 1994; this study). This may reflect increased insulin resistance in the absence of both IRS-1 and IRS-3. An additional factor contributing to hyperinsulinemia in the *Irs1*$^{-/-}$/*Irs3*$^{-/-}$ double knockout mice may be the reduced plasma leptin levels, because leptin has been shown to negatively regulate insulin secretion as part of the adipoinsular axis (Kulkarni et al. 1997; Kieffer and Habener 2000).

The *Irs1*$^{-/-}$/*Irs3*$^{-/-}$ double knockout mouse represents a novel model of lipoatrophic diabetes. It shares many of the metabolic characteristics common to patients and other transgenic mouse models of this disorder, including hyperglycemia, hyperinsulinemia, insulin resistance, and glucose intolerance (Reitman et al. 2000). However, the *Irs1*$^{-/-}$/*Irs3*$^{-/-}$ double knockout mice do not exhibit the increased fat in liver or muscle that is observed in most other forms of lipoatrophic diabetes. The hyperglycemia and hyperinsulinemia of the *Irs1*$^{-/-}$/*Irs3*$^{-/-}$ double knockout mice are reversed by adenovirus-mediated expression of leptin in the liver. This shows that, although IRS-1 and IRS-3 are missing from all tissues, a major factor in development of the diabetic phenotype is

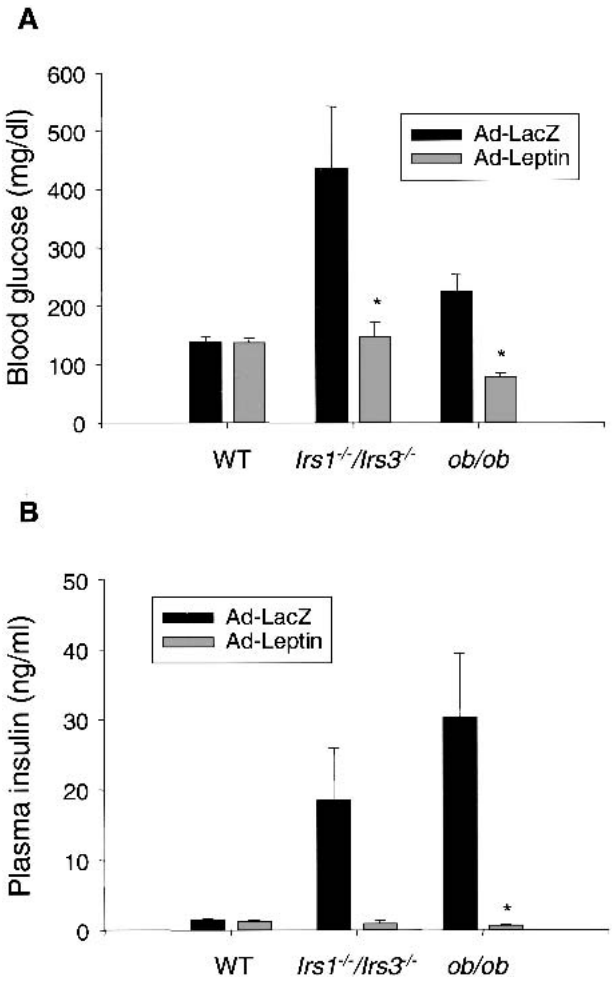

Figure 7. Reversal of diabetes by leptin in $Irs1^{-/-}/Irs3^{-/-}$ double knockout mice. (*A*,*B*) Blood glucose levels (*A*) and plasma insulin levels (*B*) were determined in wild-type, $Irs1^{-/-}/Irs3^{-/-}$ double knockout, and *ob*/*ob* mice 6 d after injection of 5×10^8 PFU/g body weight of adenovirus carrying cDNA coding for either leptin (Ad-Leptin) or β-galactosidase (Ad-LacZ). Each bar represents the mean ± S.E. for four animals, except for the bar representing *ob*/*ob* mice injected with Ad-LacZ, in which n = 3. *, $P < 0.05$ Ad-Leptin-treated mice versus corresponding Ad-LacZ-treated mice.

the deficiency in adipose tissue and the associated decreased level of adipose-derived leptin. Exogenous leptin has also been shown to rescue diabetes in other mouse models of lipoatrophic diabetes (Shimomura et al. 1999; Gavrilova et al. 2000; Ebihara et al. 2001). In a recent clinical study involving fat-deficient patients, leptin replacement therapy also led to significant metabolic improvements, confirming the clinical relevance of these findings (Oral et al. 2002).

Examination of the human genome for an *IRS3* gene has shown that humans lack a functional *IRS3* gene, with two large deletions including the PTB domain and with an in-frame stop codon in the remaining coding sequence. Moreover, the IRS-3 protein is undetectable in human adipocytes (G.E. Lienhard, J.R. Zierath, and S.I. Taylor, unpubl.). To the extent one can extrapolate from mice to humans, this lack of IRS-3 in humans might produce an increased dependence on IRS-1 in both adipocyte differentiation and control of insulin sensitivity. If this is the case, then mutations or sequence variants of IRS-1 such as those reported in a number of studies (Almind et al. 1993; Imai et al. 1994; Laakso et al. 1994; Whitehead et al. 1998) may lead to more exaggerated effects than would occur if IRS-3 were also present.

In conclusion, we have shown that combined deficiency of IRS-1 and IRS-3 results in severe deficiency of white adipose tissue, providing evidence that IRS-1 and IRS-3 are complementary in their roles in adipogenesis. This double knockout also results in a unique form of lipoatrophic diabetes. In contrast, the $Irs1^{-/-}/Irs4^{-/-}$ double knockout mice were, to the extent studied, indistinguishable from $Irs1^{-/-}$ mice in terms of growth, development, and glucose homeostasis. These findings indicate that there is no functional overlap between IRS-1 and IRS-4 with respect to regulation of these parameters, leaving the physiological role of IRS-4 to be determined.

Materials and methods

Animals and genotyping

The generation of mice with targeted disruption of *Irs1*, *Irs3*, or *Irs4* has been described previously (Araki et al. 1994; Liu et al. 1999; Fantin et al. 2000). Mice were housed on a 12-h light, 12-h dark cycle. For the IRS-1/IRS-3 study, mice were fed Mouse Diet 9F (PMI Nutrition International), and for the IRS-1/IRS-4 study, mice were kept on Teklad LM-485 mouse/rat diet (Harlan Teklad). Genotyping was performed by PCR analysis of genomic DNA obtained from tail snips. For each *Irs*, the PCR reaction mixture contained three primers: primer 1 was located in the DNA common to the wild-type and the knockout at a site just 5′ to the *neo* gene in the knockout; primer 2 was located in the wild-type gene at a site just 3′ to where it was interrupted in the knockout; and primer 3 was located in the *neo* gene of the knockout at a 5′ site of the *neo* gene. The PCR mixtures thus gave the primer ½ product from the *Irs* gene and the primer ⅓ product from the knockout. This allowed us to distinguish between the *neo* gene replacing one *Irs* from the *neo* gene replacing the second *Irs*, and thus to determine whether a mouse was heterozygous for both or one *Irs* gene. The detailed protocols for the genotyping will be furnished on request. *ob*/*ob* mice were obtained from Jackson Laboratory. All procedures involving animals were approved by the Animal Care Committees of the Joslin Diabetes Center or Dartmouth Medical School.

Analytical procedures

For the IRS-1/IRS-3 study, blood glucose levels were measured from whole venous blood using an automatic glucometer (Glucometer Elite, Bayer). Plasma insulin levels were determined by ELISA using mouse insulin as a standard (Crystal Chem). Plasma leptin levels were measured by ELISA using mouse leptin as a standard (Crystal Chem). Triglyceride levels in plasma from fasted animals were determined using the GPO-Trinder Assay (Sigma). Plasma free fatty acid levels in fasted animals were measured using the NEFA-Kit-U (Amano). For glucose tol-

erance tests (GTT), animals were fasted overnight (16 h), after which glucose was injected intraperitoneally (2 g/kg body weight) and glucose levels were determined at the indicated time points. Insulin tolerance tests (ITT) were performed on random-fed mice by intraperitoneal injection of 1 U/kg body weight human insulin (Eli Lilly). Glucose levels were measured immediately before and at the indicated time points after injection. Body triglyceride content was determined by enzymatic measurement (GPO-Trinder, Sigma) of glycerol after decomposition of whole carcasses in ethanolic KOH. For determination of tissue triglyceride content, tissue pieces (50–100 mg) were homogenized on ice in TAG buffer (50 mM Tris, 100 mM KCl, 20 mM NaF, 0.5 mM EDTA, 0.05% C12E9 at pH 8.0). Following centrifugation, glycerol content of the supernatant was determined using the GPO-Trinder assay (Sigma).

For the IRS-1/IRS-4 study, blood glucose levels were measured with the Precision G blood glucose testing system (Medisense). Plasma insulin levels were determined using an insulin radioimmunoassay (Linco Research). GTT and ITT were performed as described above, except for the insulin dose for the ITT, which was 0.75 U/kg body weight.

Northern blot

Total RNA was prepared from isolated epididymal fat pads using Trizol reagent (GIBCO-BRL). Transfer of RNA to nylon membranes and hybridization with a ^{32}P-labeled PPARγ cDNA probe were according to standard protocols.

Histology

Tissues were fixed in 10% buffered formalin and imbedded in paraffin. Multiple sections (separated by 70–80 μm each) were obtained from perigonadal fat pads and analyzed systematically with respect to adipocyte size and number. Staining of the sections was performed with hematoxylin/eosin. For each genotype at least 10 fields (representing ~100 adipocytes) per slide were analyzed. Images were acquired using a BX60 microscope (Olympus) and an HV-C20 TV camera (Hitachi) and were analyzed using Image-Pro Plus 4.0 software.

β-*cell mass*

The pancreas was rapidly dissected, weighed, and fixed in Bouin's solution for 6 h, then stored in 10% buffered formalin for at least 48 h. Following embedding in paraffin, sections of pancreas were stained for non-β-cell hormones using a cocktail of antibodies to glucagon, somatostatin, and pancreatic polypeptide (Kulkarni et al. 1999). β-cell mass was evaluated by point-counting morphometry on immunoperoxidase-stained sections of pancreas. Multiple sections (separated by 70–80 μm each) were obtained from each pancreas and analyzed systematically using a grid system covering at least 250 fields per mouse. Images were acquired using a BX60 Microscope (Olympus) equipped with a U-PMTVC video adapter (Olympus) and an HV-C20 TV camera (Hitachi) and were analyzed using Image-Pro Plus 4.0 software. Relative volumes were calculated for β-cells, non-β-cells, and exocrine tissue. Contaminating tissue (including adipose, lymph nodes, and intestines) was recorded to correct for the pancreatic weight. The β-cell mass was then calculated by multiplying the relative β-cell volume by the corrected pancreatic weight (Michael et al. 2000).

Adenovirus-mediated gene transfer

Recombinant adenovirus carrying the rat leptin cDNA under the control of the cytomegalovirus promotor was kindly provided by Christopher B. Newgard (University of Texas Southwestern Medical Center, Dallas). Adenovirus carrying the bacterial β-galactosidase gene was kindly provided by I. Saito (Tokyo University). Virus was amplified in HEK293 cells and purified through CsCl gradients as described (Miyake et al. 1996). Mice were injected with 5×10^8 plaque-forming units (PFUs) per gram body weight. Blood glucose was measured at day 6 after injection of virus. Blood for insulin assays was collected on the same day.

Statistics

All data were subjected to statistical analysis using the Student's t-test with differences between means considered significant for P values <0.05.

Acknowledgments

We thank Matthias Blüher, Joslin Diabetes Center, for valuable help and advice; Shannon E. Curtis for excellent technical assistance; Christopher B. Newgard for providing the leptin adenovirus; and I. Saito for providing the LacZ adenovirus. This work was supported by a Juvenile Diabetes Research Foundation Postdoctoral Fellowship (to P.G.L.), DK 02885-KO8 Clinical Scientist Award (to R.N.K.), and NIH grants DK 42816 (to G.E.L.) and DK 33201 (to C.R.K.), as well as the Joslin DERC grant (DK 57521).

The publication costs of this article were defrayed in part by payment of page charges. This article must therefore be hereby marked "advertisement" in accordance with 18 USC section 1734 solely to indicate this fact.

References

Almind, K., Bjorbaek, C., Vestergaard, H., Hansen, T., Echwald, S., and Pedersen, O. 1993. Amino acid polymorphisms of insulin receptor substrate-1 in non-insulin-dependent diabetes mellitus. *Lancet* **342:** 828–832.

Araki, E., Lipes, M.A., Patti, M.E., Bruning, J.C., Haag III, B., Johnson, R.S., and Kahn, C.R. 1994. Alternative pathway of insulin signalling in mice with targeted disruption of the IRS-1 gene. *Nature* **372:** 186–190.

Ebihara, K., Ogawa, Y., Masuzaki, H., Shintani, M., Miyanaga, F., Aizawa-Abe, M., Hayashi, T., Hosoda, K., Inoue, G., Yoshimasa, Y., et al. 2001. Transgenic overexpression of leptin rescues insulin resistance and diabetes in a mouse model of lipoatrophic diabetes. *Diabetes* **50:** 1440–1448.

Fantin, V.R., Lavan, B.E., Wang, Q., Jenkins, N.A., Gilbert, D.J., Copeland, N.G., Keller, S.R., and Lienhard, G.E. 1999. Cloning, tissue expression, and chromosomal location of the mouse insulin receptor substrate 4 gene. *Endocrinology* **140:** 1329–1337.

Fantin, V.R., Wang, Q., Lienhard, G.E., and Keller, S.R. 2000. Mice lacking insulin receptor substrate 4 exhibit mild defects in growth, reproduction, and glucose homeostasis. *Am. J. Physiol. Endocrinol. Metab.* **278:** E127–E133.

Fasshauer, M., Klein, J., Ueki, K., Kriauciunas, K.M., Benito, M., White, M.F., and Kahn, C.R. 2000. Essential role of insulin receptor substrate-2 in insulin stimulation of Glut4 translocation and glucose uptake in brown adipocytes. *J. Biol. Chem.* **275:** 25494–25501.

Fasshauer, M., Klein, J., Kriauciunas, K.M., Ueki, K., Benito, M., and Kahn, C.R. 2001. Essential role of insulin receptor substrate 1 in differentiation of brown adipocytes. *Mol. Cell. Biol.* **21:** 319–329.

Flier, S.N., Kulkarni, R.N., and Kahn, C.R. 2001. Evidence for a circulating islet cell growth factor in insulin-resistant states. *Proc. Natl. Acad. Sci.* **98:** 7475–7480.

Gavrilova, O., Marcus-Samuels, B., Leon, L.R., Vinson, C., and Reitman, M.L. 2000. Leptin and diabetes in lipoatrophic mice. *Nature* **403:** 850–851.

Imai, Y., Fusco, A., Suzuki, Y., Lesniak, M.A., D'Alfonso, R., Sesti, G., Bertoli, A., Lauro, R., Accili, D., and Taylor, S.I. 1994. Variant sequences of insulin receptor substrate-1 in patients with noninsulin-dependent diabetes mellitus. *J. Clin. Endocrinol. Metab.* **79:** 1655–1658.

Kieffer, T.J. and Habener, J.F. 2000. The adipoinsular axis: Effects of leptin on pancreatic β-cells. *Am. J. Physiol. Endocrinol. Metab.* **278:** E1–E14.

Kubota, N., Tobe, K., Terauchi, Y., Eto, K., Yamauchi, T., Suzuki, R., Tsubamoto, Y., Komeda, K., Nakano, R., Miki, H., et al. 2000. Disruption of insulin receptor substrate 2 causes type 2 diabetes because of liver insulin resistance and lack of compensatory β-cell hyperplasia. *Diabetes* **49:** 1880–1889.

Kulkarni, R.N., Wang, Z.L., Wang, R.M., Hurley, J.D., Smith, D.M., Ghatei, M.A., Withers, D.J., Gardiner, J.V., Bailey, C.J., and Bloom, S.R. 1997. Leptin rapidly suppresses insulin release from insulinoma cells, rat and human islets and, in vivo, in mice. *J. Clin. Invest.* **100:** 2729–2736.

Kulkarni, R.N., Winnay, J.N., Daniels, M., Bruning, J.C., Flier, S.N., Hanahan, D., and Kahn, C.R. 1999. Altered function of insulin receptor substrate-1-deficient mouse islets and cultured β-cell lines. *J. Clin. Invest.* **104:** R69–R75.

Laakso, M., Malkki, M., Kekalainen, P., Kuusisto, J., and Deeb, S.S. 1994. Insulin receptor substrate-1 variants in non-insulin-dependent diabetes. *J. Clin. Invest.* **94:** 1141–1146.

Liu, S.C., Wang, Q., Lienhard, G.E., and Keller, S.R. 1999. Insulin receptor substrate 3 is not essential for growth or glucose homeostasis. *J. Biol. Chem.* **274:** 18093–18099.

Michael, M.D., Kulkarni, R.N., Postic, C., Previs, S.F., Shulman, G.I., Magnuson, M.A., and Kahn, C.R. 2000. Loss of insulin signaling in hepatocytes leads to severe insulin resistance and progressive hepatic dysfunction. *Mol. Cell* **6:** 87–97.

Miyake, S., Makimura, M., Kanegae, Y., Harada, S., Sato, Y., Takamori, K., Tokuda, C., and Saito, I. 1996. Efficient generation of recombinant adenoviruses using adenovirus DNA-terminal protein complex and a cosmid bearing the full-length virus genome. *Proc. Natl. Acad. Sci.* **93:** 1320–1324.

Oral, E.A., Simha, V., Ruiz, E., Andewelt, A., Premkumar, A., Snell, P., Wagner, A.J., DePaoli, A.M., Reitman, M.L., Taylor, S.I., et al. 2002. Leptin-replacement therapy for lipodystrophy. *N. Engl. J. Med.* **346:** 570–578.

Reitman, M.L., Arioglu, E., Gavrilova, O., and Taylor, S.I. 2000. Lipoatrophy revisited. *Trends Endocrinol. Metab.* **11:** 410–416.

Rosen, E.D. and Spiegelman, B.M. 2000. Molecular regulation of adipogenesis. *Annu. Rev. Cell Dev. Biol.* **16:** 145–171.

Saltiel, A.R. and Kahn, C.R. 2001. Insulin signalling and the regulation of glucose and lipid metabolism. *Nature* **414:** 799–806.

Sciacchitano, S. and Taylor, S.I. 1997. Cloning, tissue expression, and chromosomal localization of the mouse IRS-3 gene. *Endocrinology* **138:** 4931–4940.

Shimomura, I., Hammer, R.E., Ikemoto, S., Brown, M.S., and Goldstein, J.L. 1999. Leptin reverses insulin resistance and diabetes mellitus in mice with congenital lipodystrophy. *Nature* **401:** 73–76.

Tamemoto, H., Kadowaki, T., Tobe, K., Yagi, T., Sakura, H., Hayakawa, T., Terauchi, Y., Ueki, K., Kaburagi, Y., Satoh, S., et al. 1994. Insulin resistance and growth retardation in mice lacking insulin receptor substrate-1. *Nature* **372:** 182–186.

Virkamaki, A., Ueki, K., and Kahn, C.R. 1999. Protein–protein interaction in insulin signaling and the molecular mechanisms of insulin resistance. *J. Clin. Invest.* **103:** 931–943.

Whitehead, J.P., Humphreys, P., Krook, A., Jackson, R., Hayward, A., Lewis, H., Siddle, K., and O'Rahilly, S. 1998. Molecular scanning of the insulin receptor substrate 1 gene in subjects with severe insulin resistance: Detection and functional analysis of a naturally occurring mutation in a YMXM motif. *Diabetes* **47:** 837–839.

Withers, D.J., Gutierrez, J.S., Towery, H., Burks, D.J., Ren, J.M., Previs, S., Zhang, Y., Bernal, D., Pons, S., Shulman, G.I., et al. 1998. Disruption of IRS-2 causes type 2 diabetes in mice. *Nature* **391:** 900–904.